On the theory of hydrogen orderings in tantalum hydrides

1991 J. Phys.: Condens. Matter 3 4533

(http://iopscience.iop.org/0953-8984/3/25/003)

J. Phys.: Condens. Matter 3 (1991) 4533–4545. Printed in the UK

On the theory of hydrogen orderings in tantalum hydrides

V G Vaks† and V I Zinenko‡
† I V Kurchatov Institute of Atomic Energy, Moscow 123182, USSR
‡ State University of Krasnoyarsk, Krasnoyarsk 660062, USSR

Received 8 March 1990

Abstract. The model and methods developed earlier for describing the statistical properties of hydrogen in the NbH_x-type systems are used to investigate the transition between the phases α, α', β, δ and ε in TaH_x. The main features of the observed phase diagram (x, T) can be naturally explained if one assumes that the concentration dependence of the hydrogen partial enthalpy $h_H(x)$ in TaH_x has an anomaly near $x_c \simeq 0.5$ similar to that established earlier for NbH_x. Then, treating values of the mean-field constants in the ordered phases as parameters of the model we can fairly well describe all the main features of the complex phase diagram of TaH_x in the whole (x, T) range considered. We also discuss the structure of the ordered phases and the temperature dependences of the order parameters. An anomalous softening for some critical concentration waves is predicted which can be observed in neutron or x-ray diffraction experiments for the disordered α-phase.

1. Introduction

Investigations of the phase transitions (PTs) of hydrogen in the transition metal hydrides MH_x attract much attention (see, e.g., Shober and Wenzl 1978, Somenkov and Shilstein 1980). This is due to the considerable effect of these PTs on various properties of hydrides and also because the investigations of the PTs in these relatively simple systems can yield important information on the general features of the interatomic interactions and orderings in the interstitial alloys. The hydrides (and deuterides) of the niobium group metals are classic representatives of the MH_x systems and the theoretical understanding of complicated orderings and phase diagrams in these alloys can provide significant information on the bonding and H–H interactions in hydrides.

Microscopic models of the PTs in NbH_x-type alloys have been discussed by a number of workers. Horner and Wagner (1974) and Futran *et al* (1982) considered the α-to-α' PT in NbH_x of the lattice gas–lattice liquid type. Using the Monte Carlo method and a simple model of the pairwise H–H interactions equal to the sum of the stress-induced ('elastic') term V_{si} and the strong repulsion (blocking) V_{sr} in the first three coordination spheres, these workers succeeded in a fair description of the observed phase equilibrium curve $T_{\alpha\alpha'}(x)$ although at large x (>0.5) the disagreements with experiments grew. Hall *et al* (1987) discussed the PT to the ordered β- and ε-phases in NbH_x (of the MH and M_4H_3 type). They concluded that the above-mentioned model with $V_{HH} = V_{si} + V_{sr}$ is insufficient for the description of these PTs.

0953-8984/91/254533 + 13 $03.50

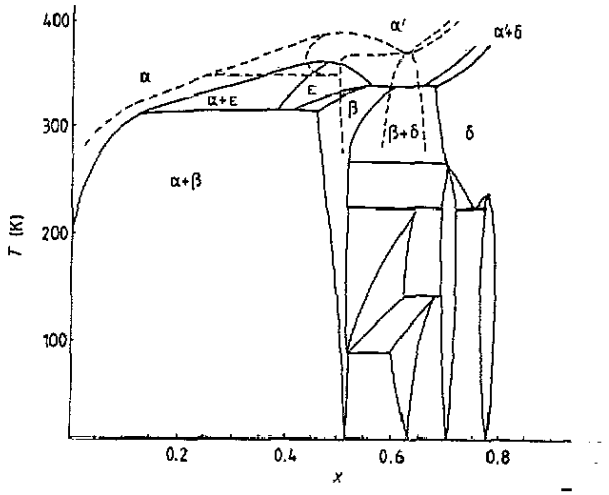

Figure 1. Phase diagram of the TaH_x system: ———, experiment (Köbler and Welter 1981); – – –, our calculation with the parameter values from equation (18).

The thermodynamic properties and PTs of hydrogen in the NbH_x-type hydrides were discussed in more detail in the papers by Vaks and Orlov (1986, 1988, hereafter referred to as I and II, respectively), Vaks and Zein (1987, hereafter referred to as III), Vaks *et al* (1984, 1988a,b hereafter referred to as IV, V and VI, respectively) and Vaks and Zinenko (1989, hereafter referred to as VII). To calculate the statistical properties these workers used an analytical cluster field method which is a simplified version of the known cluster variation method, being also suitable for allowing for long-range interactions. A number of problems and properties have been considered: the α-to-α' PT (II and IV), symmetry of the ordered phases (I and III), short-range order effects (V and VI), thermodynamic properties of the disordered α-phase (II), PT to the MH phases, i.e. to the β-phase in NbH_x and δ-phase in TaH_x and VD_x (VII), etc. It was found, in particular, in II from an analysis of the thermodynamic data of Kuji and Oates (1984a) that the partial enthalpy $h_H(x)$ of hydrogen in the α-phase of NbH_x starts to increase sharply at some $x \geqslant x_c \approx 0.6$, which apparently reflects a significant variation in the hydrogen electronic state in NbH_x at these x. This concentration anomaly of $h_H(x)$ enabled us to explain in VII the peculiar features of the phase equilibria $\alpha(\alpha')$–β in NbH_x and, in particular, the abnormally broad range of the concentration stability (from $x \approx 0.7$ to $x = 1.1$) for the ordered β-phase. Using the H–H interaction model from II and two phenomenological mean-field parameters γ_i for the β-phase we described the phase diagram and a number of characteristics of the PT in NbH_x in fair agreement with experiments (VII).

In the present paper we apply the methods and results of I–VII to investigate the PTs between the phases α, α', β, δ and ε in TaH_x, i.e. between all the high-temperature phases of these hydrides (figure 1). The phase diagram is rather complicated here and earlier it has not been discussed microscopically. Using the same approximations as in II and VII for NbH_x we show that to describe the main features of the phase diagram for TaH_x it is necessary to suppose that at some $x \approx x_c$ the hydrogen partial enthalpy $h_H(x)$ in the α-phase has a sharp concentration anomaly analogous to that observed by Kuji and Oates (1984a) for NbH_x. The estimated value $x_c^{Ta} \approx 0.5$ in TaH_x turns out to be

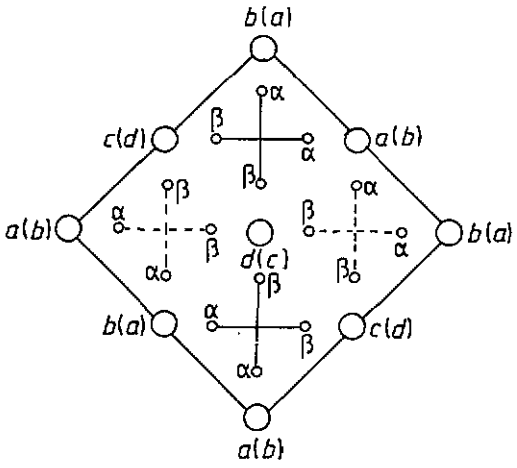

Figure 2. The M_2X ordering in the BCC hydrides (III); for clarity, metal atoms are not shown. The large open circles are tetrahedral interstitial sites in sublattices 3 and $\bar{3}$; the small open circles are those in sublattices 1, $\bar{1}$, 2 and $\bar{2}$. The full and broken lines link sites in the planes $z = 0$ and $z = \frac{1}{2}a$, respectively, where a is the BCC lattice constant. The indices a, b, c and d in (without) parentheses correspond to the sites in the plane $z = \frac{1}{4}a$ ($z = \frac{3}{4}a$). In the case of perfect ordering, only sites of type a are occupied. The structure is periodic in the $(\pm 1, \pm 1, 0)$ directions.

slightly lower than in NbH_x, which correlates with the data on the impurity electrical resistivity in TaH_x and NbH_x discussed below. Introducing further phenomenological mean-field constants γ_i to describe the interactions in the ordered phases (as was done in VII) we can obtain a good description of all the observed phase equilibria α–α'–β–δ–ε in TaH_x. We also discuss the sensitivity of the phase diagram to the model parameter variation, the stiffness values for the critical concentration waves (CWS) characterizing tendencies to various orderings (V) and the temperature dependences of the order parameters. The main conclusions and predictions of the theory are presented in section 4.

2. The model and methods of calculation

The model, approximations and ordering characteristics used were described in I–III and VII. For convenience we present the main relations. In the hydrides under consideration the hydrogen atoms occupy tetrahedral sites in the BCC lattice of a metal which form six sublattices (being equivalent in the disordered α-phase) with the following basis vectors $\boldsymbol{\rho}_p$ ($p = 1, 2, 3, \bar{1}, \bar{2}$ or $\bar{3}$)

$$\boldsymbol{\rho}_1 = \tfrac{1}{4}\boldsymbol{a}_1 + \tfrac{1}{2}\boldsymbol{a}_2 \qquad \boldsymbol{\rho}_2 = \tfrac{1}{4}\boldsymbol{a}_2 + \tfrac{1}{2}\boldsymbol{a}_3 \qquad \boldsymbol{\rho}_3 = \tfrac{1}{4}\boldsymbol{a}_3 + \tfrac{1}{2}\boldsymbol{a}_1 \qquad \boldsymbol{\rho}_{\bar{K}} = -\boldsymbol{\rho}_K. \tag{1}$$

Here $\boldsymbol{a}_i$ is the translation vector along the main crystal axis i by the BCC lattice constant $a = |\boldsymbol{a}_i|$.

As was discussed in III, all the considered phases α, β, δ and ε in TaH_x can be treated as particular cases of the general M_2X-type ordering shown in figure 2. There are six non-equivalent site types in this ordering denoted by index $\lambda = a, b, c, d, \alpha$ or β. The ordering is characterized by five order parameters η_i which correspond to five static CWS (Khachaturian 1974) and are denoted as (III and V)

$$\eta_i = \{\xi, \zeta, \rho, \sigma_1, \sigma_2\}. \tag{2}$$

The mean occupation number, n_λ for the λ-type site, and the mean occupation number

$n_p(\boldsymbol{R})$ for the sublattice p in the BCC cell with the centre $\boldsymbol{R}$ are related to the order parameters η_i as follows (III):

$$\begin{aligned} n_{a,b} &= c[1 + 2\xi + 3\sigma_1 \pm 3(\zeta + \rho)] \\ n_{c,d} &= c[1 + 2\xi - 3\sigma_1 \pm 3(\zeta - \rho)] \\ n_{\alpha,\beta} &= c(1 - \xi \pm 3\sigma_2) \end{aligned} \tag{3}$$

$$\begin{aligned} n_{3,\bar{3}}(\boldsymbol{R}) &= c[1 + 2\xi \pm 3\zeta + 3(\rho + \sigma_1)\exp(i\boldsymbol{k}_1 \cdot \boldsymbol{R})] \\ n_{1,\bar{1}}(\boldsymbol{R}) &= n_{2,\bar{2}}(\boldsymbol{R}) = c[1 - \xi \pm 3\sigma_2 \exp(i\boldsymbol{k}_1 \cdot \boldsymbol{R})]. \end{aligned} \tag{4}$$

Here the upper sign on the right-hand side of each equation corresponds to the first index on the left-hand side, and the lower sign to the second index; $c = \frac{1}{6}x$ is the mean occupation number in the MH_x alloy and $\boldsymbol{k}_1 = (1, 1, 0)\pi/a$ is the superstructure vector for the CW ρ, σ_1 or σ_2.

In TaH_x the M_2X ordering corresponds to the β-phase. At perfect ordering of this phase the order parameters are $\xi = \rho = \zeta = \sigma_1 = 1$, $\sigma_2 = 0$, and $n_a = 2x$, $n_{\lambda \neq a} = 0$. The MX ordering in TaH_x corresponds to the δ-phase in which $\zeta = \sigma_i = 0$, $n_a = n_d$, $n_b = n_c$, and at perfect ordering we have $\xi = \rho = 1$, $n_a = x$, $n_b = n_a = 0$. In accordance with the non-zero values of the order parameters, the M_2X ordering will be denoted as the (ξ, ζ, ρ, σ)-phase, and the MX ordering as the (ξ, ρ)-phase. It was shown in III that three more partially ordered phases based on M_2X ordering are thermodynamically possible:

$$\xi\text{-phase: } \xi \neq 0 \qquad \zeta = \rho = \sigma_i = 0 \tag{5a}$$

$$(\xi, \sigma)\text{-phase: } \xi \neq 0 \quad \sigma_i \neq 0 \qquad \zeta = \rho = 0 \tag{5b}$$

$$(\xi, \zeta)\text{-phase: } \xi \neq 0 \quad \zeta \neq 0 \qquad \rho = \sigma_i = 0. \tag{5c}$$

Following III, we shall assume that the ε-phase in TaH_x corresponds to (ξ, σ) ordering. This ordering corresponds to the equal occupation numbers for the sublattices a and b in figure 2, $n_a = n_b$, while in the experiments of Kaneko *et al* (1984) similar but different values, $n_a \simeq 0.6$ and $n_b \simeq 0.4$, were reported. As was discussed in III, further and more refined investigations of the phase structure seem to be desirable.

Following II, we write the free energy F for the MH_x alloy (per M atom) in the form

$$F(x, T) = F_{\text{conf}}(x, T) + E_{\text{ci}}(x) + F_{\text{ph}}(x, T) \tag{6}$$

while the chemical potential, μ, of hydrogen is $\partial F/\partial x$. In equation (6), F_{conf} is the configurational contribution to F corresponding to the energy and entropy of various H atom distributions over interstitial sites, E_{ci} is a configuration-independent term (including, in particular, the 'configurationally averaged' part of the band-structure energy) and F_{ph} is the phonon contribution.

The F_{conf}-term in (6) is calculated by the methods described in I and II. For the M_2X phase it has the form

$$F_{\text{conf}}^{M_2X} \equiv F_\beta = F_\beta^{\text{s}} + F_\beta^{\text{mf}} + F_\beta^{\text{c}}. \tag{7}$$

The corresponding contribution to the chemical potential for the λ sublattice is $\mu_\beta^\lambda = \nu_\lambda^{-1}(\partial F_\beta/\partial n_\lambda)$, where ν_λ is the number of λ-type sites per M atom ($\nu_{a,b,c,d} = \frac{1}{2}$, $\nu_{\alpha,\beta} = 2$). F^{s} in equation (7) is the contribution to F from the configurational entropy and from the H–H interactions in the three first coordination spheres V_1, V_2, V_3. This contribution is described in the '8s cluster approximation' discussed in I and II. For the

model used with blocking in two coordination spheres (V_1, $V_2 \geqslant T$, V_3 is arbitrary) the expressions for F^s and corresponding chemical potentials μ_λ^s (being slightly cumbersome) are given by equations (29) and (32) in I. The F^{mf}-term in (7) is the contribution from the long-range interactions $V_i \geqslant 4$ described in the mean-field approximation:

$$F_\beta^{mf}(\eta_i) = 6c^2(\tfrac{1}{2}\gamma_\alpha + \xi^2\gamma_\xi + \tfrac{3}{2}\zeta^2\gamma_\zeta + \tfrac{3}{2}\rho^2\gamma_\rho + \tfrac{3}{2}\sigma_1^2\gamma_{11}^\sigma + 3\sqrt{2}\sigma_1\sigma_2\gamma_{12}^\sigma + 3\sigma_2^2\gamma_{22}^\sigma) \tag{8}$$

where γ_i is the mean-field constant corresponding to the order parameter η_i (see V). The chemical potentials $\mu_\lambda^{mf} = \nu_\lambda^{-1}\,[\partial F^{mf}(\eta_i)/\partial n_\lambda]$ are found from equation (8) using equations (3) for $n_\lambda(\eta_i)$. The 'correlative' term F^c in equation (7) and the corresponding μ_λ^c are the differences between the contributions from the $V_i \geqslant 4$ interactions to F and μ_λ calculated in the pair cluster approximation and that in the mean-field approximation:

$$F_\beta^c = \tfrac{1}{2}\sum_{\lambda,\rho}\nu_\lambda \sum_{i=4}^{i_{max}} m_i^{\lambda\rho} F_{i,\lambda\rho}^c \qquad \mu_\lambda^c = \sum_\rho \sum_{i=4}^{i_{max}} m_i^{\lambda\rho}\,\mu_{i,\lambda\rho}^c \tag{9a}$$

$$\beta F_{i,\lambda\rho}^c = 2n_\lambda \ln(1 - n_\rho g_i^{\lambda\rho}) - \ln(1 - n_\lambda n_\rho g_i^{\lambda\rho}) - n_\lambda n_\rho \beta V_i \tag{9b}$$

$$\beta\mu_{i,\lambda\rho}^c = \ln(1 - n_\rho g_i^{\lambda\rho}) - \beta n_\rho V_i. \tag{9c}$$

Here $\beta = 1/T$, the function $g_i^{\lambda\rho}$ is

$$g_i^{\lambda\rho} = 2f_i[1 + (n_\lambda + n_\rho)f_i + R_i^{\lambda\rho}]^{-1} \qquad f_i = \exp(-\beta V_i) - 1$$
$$R_i^{\lambda\rho} = [(1 + n_\lambda f_i + n_\rho f_i)^2 - 4n_\lambda n_\rho f_i(1 + f_i)]^{1/2} \tag{10}$$

and $m_i^{\lambda\rho}$ is the number of sites of type ρ in the ith coordination sphere of site λ; $m_i^{\lambda\rho}$ obey the relation

$$\nu_\lambda m_i^{\lambda\rho} = \nu_\rho m_i^{\rho\lambda}. \tag{11}$$

The non-zero $m_i^{\lambda\rho}$ values with $\lambda \leqslant \rho$ (assuming that $\alpha < \beta < a < b < c < d$) and the total coordination numbers m_i (equal to the sum of $m_i^{\lambda\rho}$ over ρ) are presented in table 1. For $\lambda > \rho$, $m_i^{\lambda\rho}$ can be found from equation (11).

The H–H interaction constants $V_i = V_{HH}(r_i)$ were calculated from the model described in II in which V_{HH} is the sum of the stress-induced term V_{si}, the anharmonic repulsion V_{sr} in three first coordination spheres and the screened Coulomb ('electronic') interaction V_e of protons. These V_i are presented in table 1. The mean-field constants γ_i in (8) corresponding to this model were calculated by the method, described in V for NbH_x, and are (in kelvins, here and below)

$$\gamma_\alpha = -7100 \qquad \gamma_\xi = -2300 \qquad \gamma_\zeta = -4700 \qquad \gamma_\rho = -300$$
$$\gamma_{11}^\sigma = -3900 \qquad \gamma_{12}^\sigma = -4100 \qquad \gamma_{22}^\sigma = -1700. \tag{12}$$

As was discussed in II and VII, to describe the observed thermodynamical properties and phase diagram of NbH_x it is necessary to allow for the sharp concentration dependence of the configuration-independent contribution $E_{ci}(x)$ in equation (6). The total temperature-independent contribution $h_{ti}^E(x)$ to the excess chemical potential $\mu^E = \mu - \mu_{id}$ (where μ_{id} is the chemical potential for the ideal solution) is

$$h_{ti}^E(x) = h_{ci}^E(x) + \mu^{mf}(x) = (\partial/\partial x)E_{ci} + \tfrac{1}{8}\gamma_\alpha x. \tag{13}$$

The $h_{ti}^E(x)$ function for NbH_x was estimated in II and VII from the data of Kuji and Oates (1984a, b) on the hydrogen solubility in NbH_x over a broad range of x. These data revealed the presence of a sharp anomaly in $h_{ti}^E(x)$, its sharp increase at $x \geqslant x_c \simeq 0.6$.

Table 1. Coordination numbers $m_i^{\lambda\nu}$ in equation (9*a*) and interaction constants $V_i = V(r_i)$ used for TaH_x.

i	$4r_{i/a}$	m_i	Non-zero $m_i^{\lambda\nu}$ with $\lambda \leqslant \nu$ (denoted as $\lambda\nu$)	V_i (K)
1	101	4	$\alpha\alpha = \alpha a = \alpha b = \beta\beta = \beta c = \beta d = 1$	∞
2	002	2	$\alpha\alpha = \alpha\beta = \beta\beta = 1$; $ab = cd = 2$	∞
3	211	8	$\alpha\alpha = \beta\beta = 4$; $\alpha a = \alpha b = \alpha c = \alpha d = \beta a = \beta b = \beta c = \beta d = 1$	800
4	220	4	$\alpha\alpha = \alpha\beta = \beta\beta = ab = ac = bd = cd = 2$	135
5	301	8	$\alpha\alpha = \alpha\beta = \beta\beta = 2$; $\alpha a = \alpha b = \alpha c = \alpha d = \beta a = \beta b = \beta c = \beta d = 1$	−43
6	222	8	$\alpha\alpha = \alpha\beta = \beta\beta = aa = ad = bb = bc = cc = dd = 4$	−174
7	123	16	$\alpha\beta = 8$; $\alpha a = \alpha b = \alpha c = \alpha d = \beta a = \beta b = \beta c = \beta d = 2$	−90
8a	004	2	$\alpha\beta = aa = bb = cc = dd = 2$	−394
8b	400	4	$\alpha\alpha = \alpha\beta = \beta\beta = 2$; $ad = bc = 4$	163
9a	033	4	$\alpha\alpha = \alpha\beta = \alpha c = \alpha d = \beta\beta = \beta a = \beta b = 1$	278
9b	141	8	$\alpha\alpha = \alpha\beta = \alpha c = \alpha d = \beta\beta = \beta a = \beta b = 2$	358
10a	402	4	$\alpha\alpha = \beta\beta = ac = bd = 4$	−160
10b	042	4	$\alpha\beta = ac = bd = 4$	597
11	323	8	$\alpha\alpha = \beta\beta = 4$; $\alpha a = \alpha b = \alpha c = \alpha d = \beta a = \beta b = \beta c = \beta d = 1$	−70
12	224	8	$\alpha\alpha = \alpha\beta = \beta\beta = ab = ac = bd = cd = 4$	74
13a	501	16	$\alpha\alpha = \alpha\beta = \beta\beta = 2$; $\alpha a = \alpha b = \alpha c = \alpha d = \beta a = \beta b = \beta c = \beta d = 1$	86
13b	413	16	$\alpha\alpha = \alpha\beta = \beta\beta = 4$; $\alpha a = \alpha b = \alpha c = \alpha d = \beta a = \beta b = \beta c = \beta d = 2$	74
15	251	16	$\alpha\beta = 8$; $\alpha a = \alpha b = \alpha c = \alpha d = \beta a = \beta b = \beta c = \beta d = 2$	125
16a	404	8	$\alpha\alpha = \alpha\beta = \beta\beta = 4$; $ab = bc = 8$	125
16b	440	4	$\alpha\beta = aa = bb = cc = dd = 4$	−31
17a	053	8	$\alpha\alpha = \alpha\beta = \alpha c = \alpha d = \beta\beta = \beta a = \beta b = 2$	132
17b	433	8	$\alpha\alpha = \alpha\beta = \alpha a = \alpha b = \beta\beta = \beta c = \beta d = 2$	−38
18a	006	2	$\alpha\alpha = \alpha\beta = \beta\beta = 1$; $ab = cd = 2$	−111
18b	442	8	$\alpha\alpha = \alpha\beta = \beta\beta = 4$; $ab = cd = 8$	−68

We are not aware of such data for TaH_x. However, the similarity of the structural and electronic properties of TaH_x and NbH_x as well as the peculiarities of their phase diagrams discussed below make it possible to suggest that the forms of the h_{ti}^{E}-functions in TaH_x and NbH_x are similar. Therefore, for qualitative considerations of the phase equilibria in TaH_x, we shall use a model 'similarity hypothesis' for $h_{ti}^{E}(x)$, supposing that

$$h_{ti}^{E,Ta}(x) = \alpha[h_{ti}^{E,Nb}(x + \Delta) - h_{ti}^{E,Nb}(\Delta)]. \tag{14}$$

Here $h_{ti}^{E,Nb}(x)$ is the $h_{ti}^{E}(x)$-function for NbH_x given by equation (29*b*) in II, α characterizes a scale and Δ is a shift of the anomaly position in $h_{ti}^{E}(x)$. The subtraction of the second term in square brackets in equation (14) ensures the fulfilment of the equality $h_{ti}^{E}(0) = 0$ following the definition of $h_{ti}^{E}(x)$. Let us note that when the $h_{ti}^{E,Nb}(x)$-function is linear, e.g. when $h_{ti}^{E,Nb}(x)$ includes only the mean-field term $\mu^{mf} = \frac{1}{6}\gamma_\alpha x$, then the expression in square brackets in (14) coincides with the $h_{ti}^{E,Nb}(x)$-function itself. Thus the shift Δ is significant only for non-linear contributions to $h_{ti}^{E}(x)$. In estimating the parameter α in (14) we take into account that the mean-field constant γ_α in equation (13) for NbH_x exceeds noticeably that for TaH_x (II). Therefore, one may suppose that the total $h_{ti}^{E,Ta}(x)$ is smaller in magnitude than $h_{ti}^{E,Nb}(x)$, i.e. $\alpha < 1$ in equation (14). In estimating the shift Δ one can take into account the correlation

(discussed in II) between the position x_c of the $h_{ti}^{E,Nb}(x)$ anomaly and that of the maximum in the impurity electrical resistivity $\Delta\rho_H(x)$ (Welter and Shöndube 1983). It can imply that both the anomalies have the same origin: a sharp change in the hydrogen electronic state in NbH_x at $x \simeq x_c \simeq 0.6$. An analogous maximum in $\Delta\rho_H(x)$ for TaH_x is observed at lower $x \simeq 0.5$ (Pryde and Tsong 1971). Therefore, one can suppose that the $h_{ti}^{E}(x)$ anomaly position for TaH_x is shifted to lower x relative to $x_c^{Nb} \simeq 0.6$, i.e. that $\Delta \simeq 0.1$ in equation (14).

We are also not aware of data on the phonon spectra for TaH_x the concentration dependence of which determines the $F_{ph}(x, T)$-contribution in (6). However, this contribution affects the PT under consideration much more weakly than $E_{ci}(x)$ (II). To be definite, we shall assume by analogy with equation (14) that

$$F_{ph}^{Ta}(x, T) - F_{ph}^{Ta}(0, T) = \alpha[F_{ph}^{Nb}(x, T) - F_{ph}^{Nb}(0, T)] \tag{15}$$

with the same α as in (14) and $F_{ph}^{Nb}(x, T)$ given by equations (4) and (26) in II.

For the given x and T, the order parameter equilibrium values η_i^e can be found either from the equality condition for the sublattice chemical potentials

$$\mu_a = \mu_b = \mu_c = \mu_d = \mu_\alpha = \mu_\beta \tag{16}$$

or from the equivalent condition of the free-energy $F(x, T, \eta_i)$ minimum over η_i. As in VII, we used the second method and minimized $F(\eta_i)$ in the five-dimensional region $0 \leqslant \eta_i \leqslant 1$ on a mesh of the η_i-values with some $\Delta\eta_i$ steps. The value $\Delta\eta_i = 0.05$ was usually employed. The testing calculations with a smaller $\Delta\eta_i = 0.03$ revealed that at $\Delta\eta_i = 0.05$ the computation accuracy for the phase equilibrium curves $T_{jk}(x)$ was several per cent.

The temperatures $T_{jk}(x)$ for equilibrium between j- and k-phases were determined from the usual equations

$$\mu_j(T, x_j, \eta_i^{ej}) = \mu_k(T, x_k, \eta_j^{ek}) \tag{17a}$$

$$\Omega_j(T, x_j, \eta_i^{ej}) = \Omega_k(T, x_k, \eta_j^{ek}). \tag{17b}$$

Here $\Omega_j = F_j + x_j\mu_j$ is the thermodynamic potential for the phase j, $\eta_i^{ej} = \eta_i^{ej}(x_j, T)$ is the equilibrium order parameter in this phase, and x_j and x_k are the boundary concentrations for the region in which j and k phase coexist in the (x, T) diagram. In accordance with figure 1, we considered equilibria between the following phases:

$$(j\text{–}k) \equiv (\alpha\text{–}\beta), (\alpha\text{–}\varepsilon), (\varepsilon\text{–}\beta), (\beta\text{–}\delta), (\varepsilon\text{–}\alpha'), (\alpha'\text{–}\delta).$$

In addition we considered also equilibria with the ξ- and (ξ, ζ)-phases defined by equations (5*a*) and (5*c*) which arose in the calculations at some values of the model parameters.

3. Phase diagram and characteristics of orderings

As in VII, in the present calculations of the phase diagram the mean-field constants γ_i in equation (8) will be treated as model parameters which can also include contributions (e.g. those of the band-structure variations) disregarded in the simple model in section 2 with $V_{HH} = V_{si} + V_{sr} + V_e$. The γ_i-values for TaH_x in the model presented in equation (12) are similar to those calculated in the same model for NbH_x (in model A in V). It is noted in VII that the γ_ξ-values appear to be realistically estimated in that model while

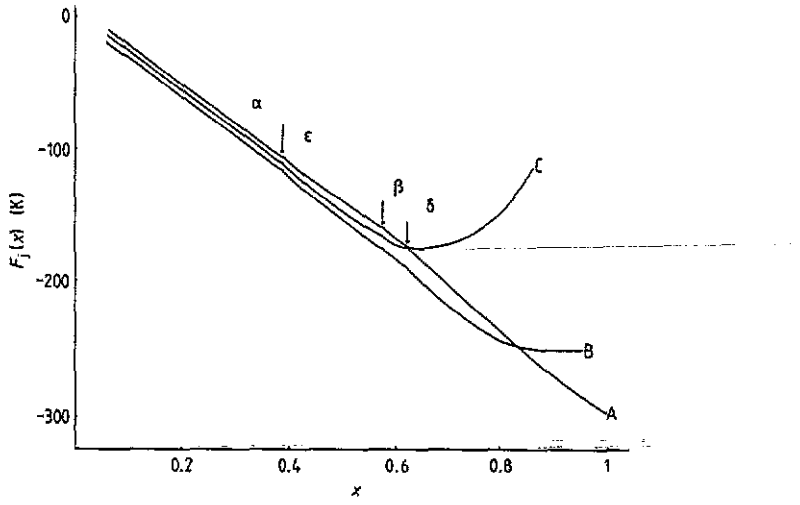

Figure 3. Concentration dependence of free energies $F_j(x)$ for the phases $j \equiv \alpha, \beta, \delta$ and ε in TaH_x at $T = 360$ K calculated in models with γ_i from equation (18) and using various $h_{ii}^{E}(x)$ in equation (13): curve A, $h_{ci}^{E} = 0$, $h_{ii}^{E} = \mu^{mf}(x)$; curve B, $h_{ii}^{E} = h_{ii}^{E,Nb}(x)$; curve C, $h_{ii}^{E} = h_{ii}^{E,Ta*}(x)$ from equation (14) with $\alpha = 0.8$, $\Delta = 0.1$.

the $|\gamma_\rho|$-values are abnormally small and seem to be underestimated significantly. In the phase diagram calculations with such γ_ρ-values the emergence of the CW ρ is strongly suppressed. Thus instead of the ordered (ξ, ρ)-phase (the β-phase in NbH_x or δ-phase in TaH_x) a partially ordered ξ-phase arises which is not observed in experiments. Therefore, as in VII, we suppose that the above-mentioned effects which are absent from the model in section 2 results, in fact, in a not small $\gamma_\rho \simeq \gamma_\xi$, and in the calculation we use values close to those estimated in VII for NbH_x: $\gamma_\rho = -(1800 - 1850)$; $\gamma_\xi = -(2000 - 2200)$.

The configuration-independent contributions $E_{ci}(x)$ and $h_{ci}^{E}(x)$ in equations (16) and (13) have a considerable effect on the PT in TaH_x, as in the NbH_x case (VII). Our calculations have shown that in models with purely pairwise V_{HH} interactions, i.e. when $E_{ci} = h_{ci} = 0$, the β- and ε-phases do not emerge at any γ_i-values (equations (15) with $j \equiv \alpha$ and $k \equiv \beta$ or ε have no solutions). In addition, the δ-phase concentration stability range near the stoichiometric value $x = 1$ turns out to be quite narrow for these models: $x = 0.975$–0.995, in sharp disagreement with experiment (see figure 1). Moreover, we have found that the β- and ε-phases also do not appear if one uses the same expressions for E_{ci} and h_{ci} in TaH_x and NbH_x, i.e. if one puts $\Delta = 0$ in equation (14) (the α-value is of less importance). The phase diagram in that case becomes similar to that calculated in VII for NbH_x (figure 3 in VII) with a broad range of δ-phase concentration stability but still without the β and ε orderings. The concentration dependence of the free energies $F_j(x)$ for this case is illustrated in figure 3 where the possibility of the j–k phase equilibrium is determined by the availability of the common tangent for the functions $F_j(x)$ and $F_k(x)$. Let us note that we have obtained the same result for the NbH_x itself, too: neither the $M_2X \equiv (\xi, \zeta, \rho, \sigma)$-phase nor the (ξ, σ)-phase emerges at any γ_i-values in the models used. Therefore, the suggestion made in III that the low-temperature phases η and θ in NbH_x (their appearance was reported by Köbler and Welter (1982) but not observed by

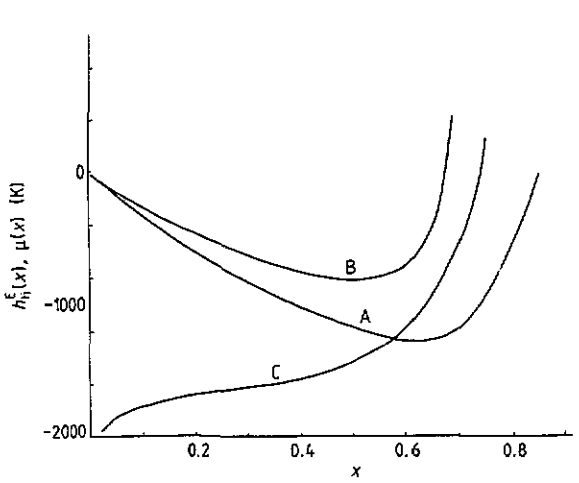

Figure 4. The function $h_{ii}^{E,Nb}(x)$ (curve A) for NbH_x given by equation (29*b*) in II, the function $h_{ii}^{E,Ta}(x)$ (curve B) for TaH_x defined by equation (14) at $\alpha = 0.8$ and $\Delta = 0.1$ and the chemical potential $\mu(x, T)$ of hydrogen (curve C) in the α-phase of TaH_x at $T = 380$ K calculated with $h_{ii}^{E,Ta}(x)$ given by curve B.

other workers) is not confirmed by the present study; our calculations do not reveal the presence of any ordered phases in NbH_x at $x \lesssim 0.6$.

In accordance with the above we described the functions $h_{ii}^{E}(x)$ in TaH_x by the model expression (14) with the values $\Delta = 0.1$ and $\alpha = 0.8$–0.6. The variation in α has a relatively weak effect on the phase diagram (compare, e.g., figures 5(*d*) and 1) and we usually used $\alpha = 0.8$. The corresponding $h_{ii}^{E}(x)$ functions for TaH_x and NbH_x are presented in figure 4.

The results of the phase diagram calculations for TaH_x with the above γ_ξ, γ_ρ and various γ_ζ, γ_{ik}^{σ} are illustrated in figures 5 and 1. If one uses the model γ_ζ, γ_{ik}^{σ}-values from equations (12) then the (ξ, ζ)-phase (denoted by symbol ζ in figure 5(*a*) and apparently not observed in real TaH_x) turns out to be stable in broad ranges of T and x which is mainly due to the large and clearly overestimated $-\gamma_\zeta$-value in equation (12). If $-\gamma_\zeta$ decreases, then only the $\beta \equiv M_2X \equiv (\xi, \zeta, \rho, \sigma)$- and the $\delta \equiv MX \equiv (\xi, \rho)$-phases appear. However, the absence of the intermediate (ξ, σ)-phase (which in TaH_x, as mentioned, corresponds apparently to the ε-phase) is characteristic of all the models with not small $-\gamma_\zeta$ and not large enough $-\gamma_{ik}^{\sigma}$. Therefore, to describe the observed phase diagram in TaH_x, one should suggest, firstly, a significantly lower $-\gamma_\zeta$-value to prevent the immediate formation of the phases comprising the ζ CW, i.e. the (ξ, ζ)- and M_2X-phases. In addition, it is necessary to assume a significant decrease in the stiffness S_{σ_-} for the 'soft' combination σ_- of the σ_1 and σ_2 CWs (defined in V), which in our model implies an increase in the $-\gamma_{ik}^{\sigma}$-values. This is illustrated in figures 5(*c*), 5(*d*), 1 and 6 which show that the intermediate (ξ, σ)-phase emerges only at rather small values of the S_{σ_-}. Let us note in this connection that, as was discussed in V, the indications of a considerable drop in the S_{σ_-}-value in the concentration region $x \simeq 0.5$ was obtained by Burkel *et al* (1981) in their x-ray diffraction experiments on NbH_x (which is a structural analogue of TaH_x).

Hence to describe the phase diagram of TaH_x we use a small $-\gamma_\zeta$ and also a large enough $-\gamma_{ik}^{\sigma}$ which correspond to the small S_{σ_-} shown in figure 6. On the whole, the

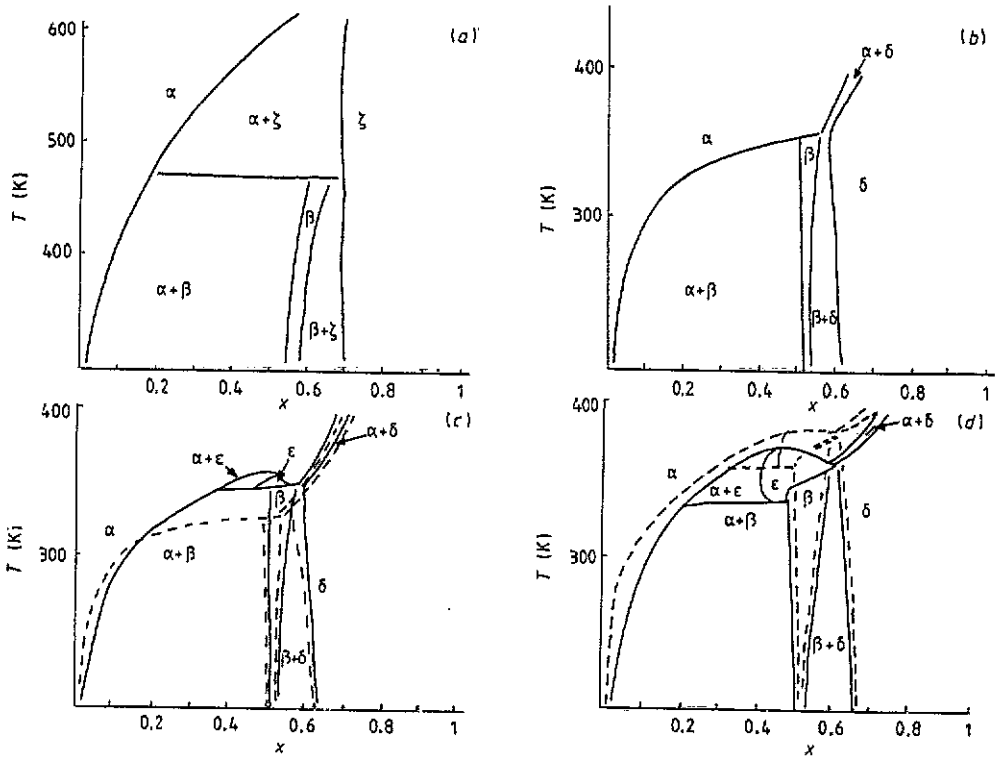

Figure 5. The phase diagrams for TaH_x calculated within the models in section 2 at $\Delta = 0.1$ and various α and γ_i. (*a*) $\alpha = 0.8$, $\gamma_\xi = -2000$, $\gamma_\rho = -1800$, γ_ζ and γ_{ik}^a are from equations (12). (*b*) $\gamma_\zeta = -2000$, the γ_i and α are the same as in (*a*). (*c*) $\alpha = 0.8$, γ_ξ, γ_ρ, γ_ζ are from equations (18): ———, $\gamma_{11}^a = \gamma_{12}^a = \gamma_{22}^a = -5900$; – – –, $\gamma_{11}^a = \gamma_{12}^a = \gamma_{22}^a = -5500$. (*d*) ———, $\alpha = 0.6$, γ_i are from equations (18); – – –, $\alpha = 0.8$, γ_ζ and γ_{ik}^a are from equations (18), $\gamma_\xi = -2200$, $\gamma_\rho = -1850$.

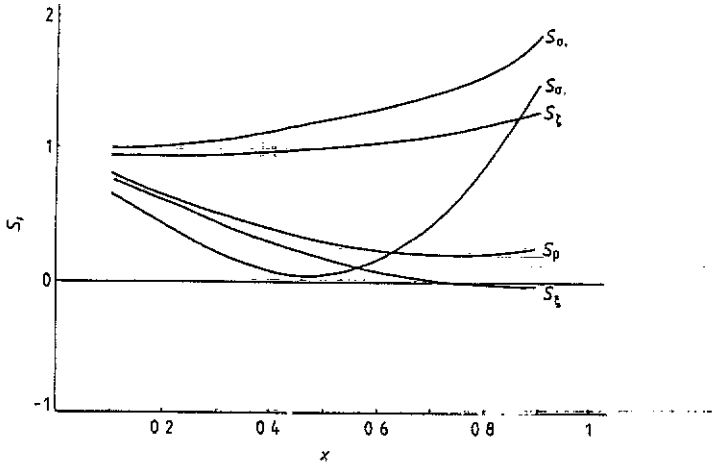

Figure 6. Concentration dependence of the CW stiffness S_i as defined by equation (8) in V: $S_i = (c^2T)^{-1}Z_i^2(\partial^2F/\partial\eta_i^2)_{\eta_i=0}$. Here c and η_i are the same as in equations (2)–(4). F is the free energy of TaH_x per Ta atom and $Z_i \simeq 1$ is a normalizing constant. The $S_i(x, T)$ functions were calculated at $T = 360$ K in the model with γ_i from equation (18).

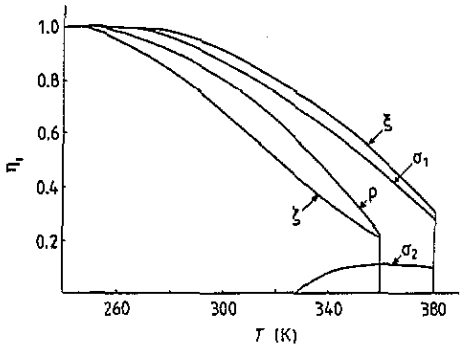

Figure 7. Temperature dependence of the order parameters $\eta_i(x, T)$ at $x = 0.55$ for the TaH_x model with γ_i from equations (18).

model used is characterized by the following parameter values:

$$\alpha = 0.8 \qquad \Delta = 0.1 \qquad \gamma_\xi = -2000 \qquad \gamma_\rho = -1800 \qquad \gamma_\zeta = -200$$
$$\gamma^\sigma_{11} = \gamma^\sigma_{22} = -6000 \qquad \gamma^\sigma_{12} = -6500. \tag{18}$$

One can use, of course, other γ_i sets satisfying the above criteria of suppressing the CW ζ and softening the CWs σ_-, ξ and ρ. However, figures 5, 6 and 1 show that the phase diagram form is rather sensitive to the choice of γ_i. Also, other phases apparently not observed in TaH_x emerge in the calculations when the γ_i are varied in too broad intervals. For example, the ξ-phase (figure 5(*a*)) appears if $-\gamma_\xi$ is large; the discussed (ξ, ζ)-phase emerges when $-\gamma_\zeta$ is not small, etc. Therefore, the scale of the γ_i magnitudes is estimated definitely enough within the model considered.

Let us still note that in the analogous description of the NbH_x phase diagram in VII at large $x \geqslant 0.8$ we also took into account a possible concentration dependence of γ_i which can arise, for example, because of the band-structure effects mentioned. However, in the present work we consider the orderings in TaH_x at not too broad a concentration range $0.4 \leqslant x \leqslant 0.7$ in which the variation in γ_i with x may be not too significant. Thus the approximation $\gamma_i(x) = \gamma_i = \text{constant}$ could be accurate enough. Figure 1 shows that, on the whole, the model used describes well all the main features of the complicated phase diagram of TaH_x in the (x, T)-region considered.

The temperature dependences of the order parameters $\eta_i(T)$ at $x = 0.55$ calculated within the model (18) are presented in figure 7. These dependences illustrate the presence of two successive PTs with decreasing temperature, first, to the (ξ, σ)-phase and, second, to the $M_2X \equiv (\xi, \zeta, \rho, \sigma)$-phase, as well as a decrease in σ_2 with decreasing T. In addition, figure 7 shows that the calculated order parameter jumps at the PTs are relatively small, i.e. these first-order PTs are close to the second-order PTs. This correlates with the considerable 'softening' of the critical ξ, ρ, σ_- CW near the PT temperatures T_c (see figures 6 and 1). Let us note, however, that the estimates of η_i in the ε-phase of TaH_x made in III from the experimental data of Kaneko *et al* (1984) yield ξ- and σ_1-values which exceed $\xi(T_c)$ and $\sigma_1(T_c)$ in figure 6 considerably: $\xi \simeq \sigma_1 \simeq 1$, $\sigma_2 \simeq 0$. Although the temperature T of the experiments of about 300 K is significantly lower than the model value of $T_c \simeq 380$ K, this discrepancy may reflect the limitations of the model and, in particular, the disregard of the electronic effects and possible concentration dependence of interactions due to these effects. Analogous disagreements have been mentioned in V in discussing the data of Burkel *et al* (1981) on the temperature-independent softening of the CWs near $x = 0.5$ in NbH_x. In this connection, further measurements of the order parameters $\eta_i(T)$ in TaH_x as well as of the CW characteristics in these hydrides (see V) seem to be rather interesting.

4. Conclusions

Let us discuss the main results and predictions of this work. As was noted in II and VII, models with pairwise concentration-independent H–H interactions can satisfactorily describe the thermodynamic properties of NbH_x and TaH_x at small concentrations $x \leqslant 0.3$. However, at certain values of $x \geqslant x_c$ the hydrogen partial enthalpy $h_H(x)$ and other characteristics of NbH_x show sharp concentration dependences which are apparently due to the changes in the hydrogen electronic state in these alloys. It was shown in VII that even a qualitative understanding of the observed phase diagram for NbH_x is hardly possible without allowing for these effects. The present study reveals that the same is apparently true for the tantalum hydrides. At the same time even taking into account these effects phenomenologically was shown to be sufficient to describe the main features of the phase diagrams. In VII this was done using the experimental data of Kuji and Oates (1984a, b) on the hydrogen solubility in NbH_x. Here we have assumed an analogous model relation (14) for TaH_x and the phase diagram calculations performed agree well with this assumption. The resulting conclusion on the peculiar form of the $h_H(x)$ function in TaH_x and, in particular, on its sharp increase in the α-phase at $x \geqslant 0.5$ (see figure 4), is an essential prediction of the theory. Its experimental verification seems to be important for the development of adequate ideas on the H–H interactions and orderings in hydrides.

The other prediction is about the structure of the ε-phase in figure 1. As was discussed in III and above, we suppose that the sublattices a and b in figure 2 are equally occupied while Kaneko *et al* (1984) had experimentally estimated $n_a \simeq 0.6$ and $n_b \simeq 0.4$. Further and more refined measurements of the n_λ-values in the ε-phase of TaH_x seem to be desirable.

One more prediction concerns the stiffness S_{σ_-} for the σ_--type CW at $x \simeq 0.5$ near the PT. It follows from our analysis that the presence of the ε-phase in TaH_x is possible only when a considerable softening of this CW in the α-phase takes place, i.e. when S_{σ_-} at these x and T decreases significantly. This must manifest itself, in particular, in a sharp increase in the x-ray or neutron scattering intensity $I(\boldsymbol{k})$ at the momentum transfer $\boldsymbol{k}$-values close to the 'critical' vector $\boldsymbol{k}_1$ in equations (3) and (4) (V). Such effects have been observed by Burkel *et al* (1981) in measurements of the x-ray scattering by NbH_x, and analogous experiments for TaH_x would be very interesting.

On the whole, the results of this and previous papers (II and VII) appear to show that all the main features of the complicated orderings and phase diagrams in NbH_x and TaH_x at the x- and T-values considered can be naturally understood in the framework of the semiphenomenological models suggested in I–VII. At the same time these considerations indicate clearly a need for further specifications of the model, in particular, in connection with the possible influence of the electronic structure on orderings

Acknowledgments

The authors are much indebted to N E Zein and V G Orlov for help with this work.

References

Burkel E, Behr H, Metzger H and Peisl J 1981 *Phys. Rev. Lett.* 46 1078

Futran M, Coates S C, Hall C K and Welch D O 1982 *J. Chem. Phys.* **77** 6223
Hall C K, Soteros C, McGillivray I and Shirley A I 1987 *J. Less-Common Met.* **130** 319
Horner H and Wagner H 1974 *J. Phys. C: Solid State Phys.* **7** 3305
Kaneko H, Kajitani T, Hirabayashi M, Niimura N, Schultz A and Leung P 1984 *J. Less-Common Met.* **103** 45
Khachaturian A G 1974 *Theory of Phase Transformations and Structure of Solid Solutions* (Moscow: Nauka)
Köbler V and Welter J-M 1982 *J. Less-Common Met.* **84** 225
Kuji T and Oates W A 1984a *J. Less-Common Met.* **102** 251
—— 1984b *J. Less. Common Met.* **102** 261
Pryde J A and Tsong I S T 1971 *Acta Metall.* **19** 1333
Shober T and Wenzl H 1978 *Hydrogen in Metals* vol 2, ed G Alefeld and J Vökkl (Berlin: Springer)
Somenkov V A and Shilstein S S 1980 *Prog. Mater. Sci.* **24** 267
Vaks V G and Orlov V G 1986 *Fiz. Tverd. Tela* **28** 3627
—— 1988 *J. Phys. F: Met. Phys.* **18** 883
Vaks V G and Zein N E 1987 *Fiz. Tverd. Tela* **29** 68
Vaks V G, Zein N E and Kamyshenko V V 1988a *J. Phys. F: Met. Phys.* **18** 1641
Vaks V G, Zein N E, Kamyshenko V V and Tkachenko Yu V 1988b *Fiz. Tverd. Tela* **30** 477
Vaks V G, Zein N E, Zinenko V I and Orlov V G 1984 *Sov. Phys.–JETP* **87** 2030
Vaks V G and Zinenko V I 1989 *J. Phys.: Condens. Matter* **1** 9085
Welter J-M and Schöndube F 1983 *J. Phys. F: Met. Phys.* **13** 529